

# Distinct Roles for Prefrontal Dopamine D1 and D2 Neurons in Social Hierarchy

Bo Xing\*, Nancy R. Mack\*, Yu-Xiang Zhang, Erin P. McEachern, and  Wen-Jun Gao

Department of Neurobiology and Anatomy, Drexel University College of Medicine, Philadelphia, Pennsylvania 19129

Neuronal activity in the prefrontal cortex (PFC) controls dominance hierarchies in groups of animals. Dopamine (DA) strongly modulates PFC activity mainly through D1 receptors (D1Rs) and D2 receptors (D2Rs). Still, it is unclear how these two subpopulations of DA receptor-expressing neurons in the PFC regulate social dominance hierarchy. Here, we demonstrate distinct roles for prefrontal D1R- and D2R-expressing neurons in establishing social hierarchy, with D1R<sup>+</sup> neurons determining dominance and D2R<sup>+</sup> neurons for subordinate. *Ex vivo* whole-cell recordings revealed that the dominant status of male mice correlates with rectifying AMPAR transmission and stronger excitatory synaptic strength onto D1R<sup>+</sup> neurons in PFC pyramidal neurons. In contrast, the submissive status is associated with higher neuronal excitability in D2R<sup>+</sup> neurons. Moreover, simultaneous manipulations of synaptic efficacy of D1R<sup>+</sup> neurons in dominant male mice and neuronal excitability of D2R<sup>+</sup> neurons of their male subordinates switch their dominant–subordinate relationship. These results reveal that prefrontal D1R<sup>+</sup> and D2R<sup>+</sup> neurons have distinct but synergistic functions in the dominance hierarchy, and DA-mediated regulation of synaptic strengths acts as a powerful behavioral determinant of intermale social rank.

**Key words:** dopamine receptors; mouse; patch clamp; prefrontal cortex; social dominance; synaptic function

## Significance Statement

Dominance hierarchy exists widely among animals who confront social conflict. Studies have indicated that social status largely relies on the neuronal activity in the PFC, but how dopamine influences social hierarchy via subpopulation of prefrontal neurons is still elusive. Here, we explore the cell type-specific role of dopamine receptor-expressing prefrontal neurons in the dominance–subordinate relationship. We found that the synaptic strength of D1 receptor-expressing neurons determines the dominant status, whereas hyperactive D2-expressing neurons are associated with the subordinate status. These findings highlight how social conflicts recruit distinct cortical microcircuits to drive different behaviors and reveal how D1- and D2-receptor enriched neurocircuits in the PFC establish a social hierarchy.

## Introduction

Dominance hierarchy widely exists across social species and significantly influences an individual animal's behavioral and social performance (Sapolsky, 2005; Wang et al., 2014; Bicks et al., 2015; Zhou et al., 2018; Matthews and Tye, 2019). Dominants take priority in accessing resources, including food, territory, and mates, whereas subordinate social status is associated with more significant social stress, which influences physical and psychological health (Blanchard et al., 2001; Bartolomucci, 2007;

Wang et al., 2014). Recent studies in humans and rodents indicate that the medial prefrontal cortex (mPFC), a brain region critical for social and cognitive functions (Bicks et al., 2015), is specifically related to social dominance (Zink et al., 2008; Chiao, 2010; Wang et al., 2011; Kingsbury et al., 2019).

Human imaging studies have shown that PFC activity is engaged with both stable and unstable hierarchies (Zink et al., 2008). In mammals, the PFC has a crucial function in decision-making and generating appropriate social responses (Rangel et al., 2008; Arnsten, 2009), although the neural mechanisms underlying the transition from unstable to stable social hierarchy remain unclear. In both primates and rodents, social hierarchy is plastic and linked to agonistic interactions, such as aggressive social behaviors between males (Rose et al., 1971; Stagkourakis et al., 2018). Once established, the hierarchy is relatively stable, preventing excessive aggressive behaviors among group-mates (Drews, 1993; Williamson et al., 2016). At the cellular level, the strength of excitatory transmission in the mPFC is one of the critical determinants of intermale hierarchy, as bidirectional manipulation of synaptic strength switched the dominance

Received Apr. 7, 2021; revised Oct. 25, 2021; accepted Oct. 27, 2021.

Author contributions: B.X. and W.-J.G. designed research; B.X., N.R.M., Y.-X.Z., and E.P.M. performed research; B.X. and N.R.M. analyzed data; B.X., N.R.M., and W.-J.G. wrote the paper.

This work was supported by National Institutes of Health R21MH110678 and R01MH085666; National Alliance for Research on Schizophrenia and Depression Independent Award 2015; and Pennsylvania Commonwealth 4100072545 (CURE 2016) to W.-J.G.

\*B.X. and N.R.M. contributed equally to this work.

The authors declare no competing financial interests.

Correspondence should be addressed to Wen-Jun Gao at wg38@drexel.edu.

<https://doi.org/10.1523/JNEUROSCI.0741-21.2021>

Copyright © 2022 the authors

relationship between males (Wang et al., 2011). The information processing and output about social competition in the mPFC fall to glutamatergic pyramidal neurons (Zhou et al., 2017). However, the pyramidal neurons in mPFC are highly heterogeneous (van Aerde and Feldmeyer, 2015). The mPFC has been implicated in diverse aspects of social behaviors, including encoding of social cues (Levy et al., 2019), social recognition processing (Phillips et al., 2019; Xing et al., 2021), and adaptive social coping (Franklin et al., 2017). It is speculated that the mPFC manages to process all these different types of social behaviors through parallel neuronal microcircuits.

Prefrontal dopamine (DA) represents an attractive target for neural influence over various social cognitive and executive functions. For example, DA in the PFC has an essential role in encoding aversive stimuli (Vander Weele et al., 2018), which may underlie enhanced avoidance and defensive behaviors in animals susceptible to social defeat stress (Ernst et al., 1997; Franklin et al., 2017). DA modulates prefrontal functions mainly through D1 receptors (D1Rs) and D2 receptors (D2Rs). The D1R- and D2R-expressing neurons in deep layers of PFC exhibit distinct electrophysiological properties, morphologic characteristics, and projection targets (Gee et al., 2012; Seong and Carter, 2012; Wei et al., 2018). Because of the different intracellular signaling pathways mediated by D1Rs and D2Rs, DA exerts divergent actions in synaptic transmission and plasticity (Xu and Yao, 2010; Tritsch and Sabatini, 2012; Xing et al., 2016a; Li et al., 2020). Indeed, activation of D1R<sup>+</sup> or D2R<sup>+</sup> neurons in the PFC plays critical but distinct roles in social information processing in rodents (Brumback et al., 2018; Shinohara et al., 2018; Xing et al., 2021) and primates (de Almeida et al., 2005; Nelson and Trainor, 2007; Lee et al., 2018). Still, the precise role of prefrontal DA signaling in the regulation of social hierarchy remains unknown. Here, we characterized the physiological properties of D1R- and D2R-expressing prefrontal neurons from dominant and subordinate mice and explored their contributions to social dominance. We found that prefrontal DA D1R<sup>+</sup> and D2R<sup>+</sup> neurons differentially control social rank, and their roles are dynamic and switchable.

## Materials and Methods

### Animals

Hemizygous *Drd1a-Cre* [stock #Tg(*Drd1a-cre*)EY262Gsat/Mmucd, GENSAT] and *Drd2-Cre* [stock #Tg(*Drd2-cre*)ER44Gsat/Mmucd, GENSAT], all on a C57BL/6J background, were bred in house to either WT C57BL/6J mice (The Jackson Laboratory) or homozygous *Ai14* mice (The Jackson Laboratory) to generate D1R-Cre, D2R-Cre, D1R-tdTomato, and D2R-tdTomato mice. Male mice 6–8 weeks of age (at the beginning of all experiments) were group-housed (2–4 per group) in a temperature- and humidity-controlled environment on a 12 h light/12 h dark cycle (light from 6:00 A.M. to 6:00 P.M.) with *ad libitum* access to food and water. The animals were cohoused during the experiments, except for the surgical and recovery period (1 week). At least 1 week before behavioral manipulations, the mice were transferred to a reverse 12 h light/dark cycle (light on from 6:00 P.M. to 6:00 A.M.), and experiments were conducted during the dark phase. All procedures were in accordance with the guidance of the National Institute of Health, and the protocols were approved by the Institutional Animal Care and Use Committee of Drexel University.

### Surgical procedure and viral gene transfer

Adult male mice were stereotaxically injected with 300 nl of viral vector as specified below. Surgical procedures were conducted under isoflurane anesthesia [4% (v/v; isoflurane/carbogen) induction, 2.5% maintenance]. Mice were placed in a stereotaxic frame (David Kopf Instruments) on a

**Table 1. Summary of viral vectors used in the experiments**

| Data     | Group             | Virus                         |
|----------|-------------------|-------------------------------|
| Figure 4 | D1Cre/inhibition  | AAV8 hSyn-DIO-hM4Di-mCherry   |
|          | D1Cre/control     | AAV8 hSyn-DIO-mCherry         |
| Figure 5 | D2Cre/inhibition  | AAV8 hSyn-DIO-hM4Di-mCherry   |
|          | D2Cre/control     | AAV8 hSyn-DIO-mCherry         |
| Figure 6 | D2Cre_subordinate | AAV8 hSyn-DIO-hM4Di-mCherry   |
|          | D1Cre_dominant    | AAV8 hSyn-DIO-hM3Dq-mCherry   |
|          |                   | AAV5-CaMKII-hChR2(H134R)-eYFP |

thermal blanket with eyes covered with artificial tears. Virus was bilaterally injected into the mPFC (anteroposterior = 1.75 mm; ML = ±0.75 mm, DV = −2.65 mm at 15° from the skull) or mediodorsal thalamus (MD) (anteroposterior = −1.4 mm; ML = ±0.5 mm, DV = −3.2 mm from the skull). For chemogenetic interventions, animals were injected with an adeno-associated virus serotype 8 (AAV8) encoding Cre-dependent human synapsin (hSyn) promoter-driven hM4D(Gi)-mCherry (Addgene 44362,  $4.6 \times 10^{12}$  GC/ml), hM3D(Gq)-mCherry (Addgene 44361,  $4.0 \times 10^{12}$  GC/ml), or -mCherry alone (Addgene 50459,  $3.8 \times 10^{12}$  GC/ml). For optogenetic stimulation experiments, we used an AAV5-CaMKII-hChR2(H134R)-eYFP (UNC Vector Core,  $5.0 \times 10^{12}$  GC per ml). The control groups were bilaterally injected with 300 nl AAV5-CaMKII-eYFP (UNC Vector Core,  $2.1 \times 10^{12}$  GC/ml). A summary of viral expression is shown in Table 1. For all injections, the virus was injected using a 32-gauge steel microinjection cannula connected via polyethylene tubing to a 1.0  $\mu$ l Hamilton syringe fitted in a motorized syringe pump (Harvard Instruments, model 11 Plus) at a flow rate of 50 nl per min. The skin was closed with sutures. Mice were given buprenorphine HCl (0.1 mg kg<sup>−1</sup>; Bedford Laboratories) and ampicillin (100 mg kg<sup>−1</sup>) for postoperative analgesia and inflammation reduction.

### Tube test for social hierarchy

To measure the dominance hierarchy in group-housed mice, the food reward-based tube tests were conducted as reported in previous studies (Wang et al., 2011; Zhou et al., 2017). Group-housed mice (2–4 per cage) were placed on a food-restricted diet consisting of 2–3 g of food (laboratory chow) per day for a week to keep 85–90% body weight before restriction. For the animals undergoing surgery, food restriction was applied when the mice recovered from surgery at least 1 week and reached body weight before surgery. A custom-made apparatus consisting of a rectangle chamber (52 cm × 25 cm × 20 cm) divided into two equal-sized compartments connected by a transparent Plexiglas tube (30 cm length and 2.5 cm inside diameter) was used for the tube test.

**Habituation session.** Mice were subjected to 2 d habituation to the test chamber. On day 1, mice were placed in the chamber with their cage mates and allowed a 5 min free exploration. Broken pieces of frosted Cheerios were used as the food reward and were scattered throughout the chamber to encourage exploration. On day 2, mice were placed in the chamber individually, and the reward was only located at each end of the tube.

**Training session.** On the subsequent 2 d (day 3 and day 4), mice underwent behavioral training consisting of eight training trials of running through the tube and consuming the food reward at the tube end in alternating directions.

**Test session.** From day 5, mice were subjected to a daily test session. Before test trials, each mouse was allowed to walk through the tube and consume the frosted Cheerios 3 times as in the training session. In the subsequent test trials, a pair of cage-mates was allowed to enter the tube from opposite ends and meet in the middle. The one that caused (pushed the other or stayed still in the tube) the other to retreat was scored as more dominant of the pair. All possible combination of pairs in each group was conducted (take 3 mice A, B, and C as an example, there are three possibilities: A-B, A-C, and B-C). The tube was cleaned with 75% ethanol after tests between cages. The start end was altered each day randomly. Social ranks were determined by the total score of the “winning-lose relationship.” The social rank between mice in a cage were considered stable when the “win-lose” relationship was identical for 3 continuous days.

### Slice electrophysiology

Similar to our prior reports (Xing et al., 2016b, 2018), acute slices of the mPFC were prepared from D1R- or D2R-tdTomato mice 24 h after a stable social hierarchy was established. Briefly, mice were deeply anesthetized with Euthasol (0.2 ml/kg, i.p.), transcardially perfused with ~20 ml ice-cold, oxygenated aCSF (in mM as follows: 128 NaCl, 2.5 KCl, 1.25 NaH<sub>2</sub>PO<sub>4</sub>, 2 CaCl<sub>2</sub>, 1 MgSO<sub>4</sub>, 26 NaHCO<sub>3</sub>, and 10 dextrose, pH 7.4) before decapitation. Coronal slices were cut on a vibratome (Leica Microsystems, VT1200S) in 300  $\mu$ m thickness and continuously perfused with oxygenated aCSF. The freshly cut slices were then warmed to 34°C for ~15 min in an oxygenated *N*-methyl-D-glucamine-based solution containing the following (in mM): 92 *N*-methyl-D-glucamine, 20 HEPES, 30 NaHCO<sub>3</sub>, 1.2 NaH<sub>2</sub>PO<sub>4</sub>, 2.5 KCl, 5 sodium ascorbate, 3 sodium pyruvate, 2 thiourea, 10 MgSO<sub>4</sub>, and 0.5 CaCl<sub>2</sub>, 10 glucose, pH 7.4 (~310 mOsm). Then, slices were transferred and maintained in oxygenated aCSF at room temperature for at least 1 h until recording.

Slices were transferred to a recording chamber where they were kept at ~34°C and superfused with ~2 ml/min oxygenated aCSF. Whole-cell current-clamp recording was used to measure basic electrophysiological properties of layer 5 D1R<sup>+</sup> and D2R<sup>+</sup> pyramidal neurons in the prelimbic (PL) region of the mPFC. The dopamine receptor expressing cells were visually identified by the presence of tdTomato by using a fluorescent microscope (Olympus BX51). A glass recording electrode (4–6 M $\Omega$  resistances) was filled with an intracellular solution containing the following (in mM): 120 K-gluconate, 20 KCl, 4 ATP-Na-ATP, 0.3 Na<sub>2</sub>GTP, 5 Na-phosphocreatine, 0.1 EGTA, 10 HEPES, pH 7.3. A series of 1500 ms current pulses (from –300 pA to 400 pA by 50 pA steps) was injected to test membrane response. All experiments were conducted with a Multiclamp 700B amplifier, a DigiData 1320 digitizer, and pClamp10.2 software (Molecular Devices). Only recordings that showed a stable resting membrane potential <–50 mV and access resistance <20 M $\Omega$  were included in the data analysis. The membrane potentials were not corrected for liquid junction potential.

The h-currents (I<sub>h</sub>) were recorded in voltage-clamp mode using a series of hyperpolarizing voltage steps (–60 mV to –130 mV by –5 mV increments) with electrodes filled with the above intracellular solution with 30 mM TEA-Cl to block delayed activated K<sup>+</sup> current (Yang et al., 2018).

For recording the evoked EPSCs, the internal solution contained the following (in mM): 120 Cs-gluconate, 5 QX-314, 6 CsCl<sub>2</sub>, 1 ATP-Mg, 0.2 Na<sub>2</sub>GTP, 10 HEPES, 5 TEA-Cl, and 0.1 spermine at pH 7.4 adjusted with CsOH. Synaptic currents were electrically evoked by stimuli (0.1 ms, 40–400  $\mu$ A at 0.05 Hz) through a concentric bipolar stimulating electrode (inner diameter: 25  $\mu$ m; outer diameter: 200  $\mu$ m, FHC) was placed in the layer 2/3 border ~300  $\mu$ m away from the recorded neurons. AMPAR-EPSCs were recorded at –60 mV, and NMDAR-EPSCs were recorded at 60 mV in voltage-clamp mode with the presence of GABA<sub>A</sub> receptor antagonist picrotoxin (50  $\mu$ M). The evoked responses of each cell were measured at –60 mV (AMPA-only response) and 60 mV (AMPA and NMDA combined response). The AMPA/NMDA ratio was calculated by dividing the amplitude of the AMPA-only response by the amplitude of the NMDA-only response was taken from a 10 ms window at 60 mV 50 ms after stimulation, where no AMPA response was present. To record the AMPA-EPSCs, the picrotoxin (50  $\mu$ M) and NMDA antagonist (R)-CPP (10  $\mu$ M) were bath-applied at least for 10 min, and then the evoked responses were measured at –60, 0, and then 60 mV. The rectification index (RI, represent current/voltage relationship) of AMPAR was calculated as the peak amplitude of AMPA–EPSC<sub>60 mV</sub>/AMPA–EPSC<sub>–60 mV</sub>.

### Chemogenetic manipulation

Water-soluble clozapine-N-oxide (CNO, Hello Bio, catalog #HB1807) was dissolved in saline at a concentration of 1 mg/ml, aliquoted, and stored at –20°C. The animal received an intraperitoneal injection of CNO at 5 mg/kg 30 min before behavioral tests.

### Optogenetic stimulation

Optical fiber-ferrule assemblies were manually made as in previous reports (Sparta et al., 2011). Bilateral ferrules were implanted 0.3 mm

above the brain regions (mPFC) for optical stimulation. Two screws were fixed into the skull to support the implant, which was secured with dental cement (Ortho-Jet). After recovery from surgery, mice were habituated to tether with the optical fiber-ferrule assemblies connected to the optical patch cables (Precision Fiber Products and ThorLabs) and a double rotary joint for 10 min twice per day over 2 d in the tube test chamber. The blue light was generated by a TTL-controlled blue light laser (473 nm, Opto Engine) at 6–8 mW. The laser output was delivered to the brain via an optical fiber (200  $\mu$ m core, 0.22 numerical aperture, Doric Lenses) which was coupled to the ferrules implanted on the animals through a zirconia sleeve. In some experiments, *in vivo* LTD induction was delivered 30 min before training sessions over 2 d: animals were injected with CNO (5 mg/kg) 30 min before the delivery of 5 ms pulses at 1 Hz for 5 min. The animals were subjected to test sessions of the tube test as described above. The implantation sites of optical fibers were verified after behavioral tests.

### Experimental designs and statistical analyses

The experimental designs are illustrated in the figures and described in the figure legends. No statistical methods were used to predetermine the sample size. For electrophysiological experiments, sample sizes were based on the number of potential identified neurons in each mouse (e.g., three cells/mouse and minimum 2 mice per group), and the number of neurons likely to yield interpretable results (10–20 neurons per condition; based on our previous studies) (Xing et al., 2016b, 2018). For behavioral experiments, sample sizes were similar to those used by others in the field (Wang et al., 2011; Zhou et al., 2017; Stagkourakis et al., 2018). Weight-matched mice were randomly assigned to groups. The investigators were not blinded to allocation during physiological experiments but were blind to outcome assessment for tube test of social hierarchy.

All statistics were calculated using GraphPad Prism 7 and or IBM SPSS 24 software. Data are presented as mean  $\pm$  SEM. Before running the *t* test or ANOVA test, deviation from normality and the homogeneity of variance tests were conducted by the Kolmogorov–Smirnov test and Levene's test, respectively. A two-tailed unpaired or paired *t* test, one- or two-way ANOVA test followed by Bonferroni's multiple comparisons was applied to all data that met these two conditions. If either the condition of equal variances or normality was not met, statistical analyses were performed using nonparametric tests. For comparison across two groups, we used the Mann–Whitney *U* test for unpaired experimental design. Comparisons across more than two groups were implemented using a Friedman test with Dunn's *post hoc* analysis. Fisher's exact test was used to determine whether there is a significant difference between two proportions of rank changes in Figure 6. In all cases, differences were considered significant at *p* values <0.05.

## Results

### Enhanced synaptic strength at D1 prefrontal neurons in dominant mice

DA signaling has a substantial influence on prefrontal synaptic activity (Tritsch and Sabatini, 2012; Xing et al., 2016a). Recent studies have indicated that AMPAR-mediated synaptic transmission in prefrontal pyramidal neurons plays a crucial role in establishing social hierarchy (Wang et al., 2011; Zhou et al., 2017). However, whether and how prefrontal neurons expressing different DA receptor subtypes (i.e., D1R- and D2R-expressing neurons) have distinct synaptic activity in dominant versus subordinate mice is unknown.

To address this question, we used a classic behavioral assay (tube test) to measure the dominant–subordinate relationship in rodents (Wang et al., 2011; Zhou et al., 2017; Stagkourakis et al., 2018) (Fig. 1A). We used a reward-based tube test to determine the dominant–subordinate relationship in a pair of mice (Fig. 1B). After group-housed mice (2 mice/group) were food-restricted, trained to walk through a narrow tube to receive food

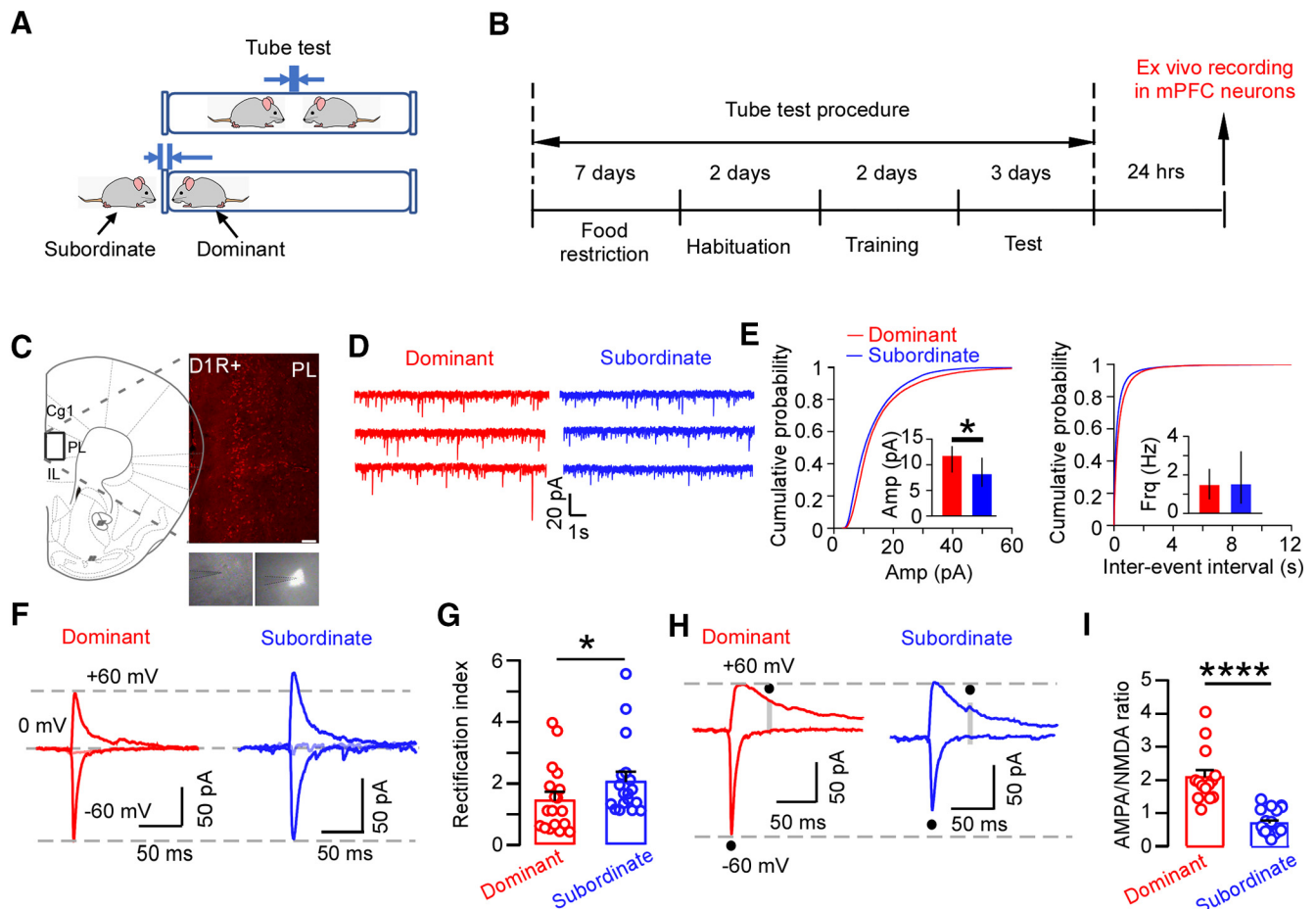


**Figure 1.** Prefrontal D1R<sup>+</sup> neurons in the dominant mice show higher AMPAR-mediated glutamate neurotransmission compared with subordinate mice. **A**, Schematic illustration of the tube test to determine the dominant and subordinate of a pair of male mice. **B**, Experimental timeline. The whole-cell patch-clamp recording was performed 24 h after the dominant–subordinate relationship was determined in the tube test. The experiments were done with the housing of 3 mice. **C**, Histologic example of PL D1R<sup>+</sup> neurons (red, tdTomato-positive). Bottom right, Differential interference contrast image of a D1R<sup>+</sup> cell (left) in PL expressing tdTomato (right). Scale bars, 200  $\mu$ m. Cg 1, Cingulate cortex, area 1; IL, infralimbic cortex. **D**, Example traces of mEPSC recordings of D1R<sup>+</sup> cells from dominant (red,  $n = 5$  mice) and subordinate (blue,  $n = 5$  mice) mice. **E**, Cumulative distributions of mEPSC amplitude (left) and interevent interval (right) for dominant (red) and subordinate (blue) mice. Insets, Mean ( $\pm$  SEM) mEPSC amplitude (left, Mann–Whitney test,  $U = 241$ ,  $*p = 0.0142$ ) and interevent interval (right, Mann–Whitney test,  $U = 377.5$ ,  $p = 0.8307$ ). **F**, Sample traces of AMPA-EPSCs recorded at  $-60$ ,  $0$ , and  $+60$  mV, respectively, in the presence of picrotoxin ( $50 \mu$ M) to block the GABA<sub>A</sub>R-mediated IPSCs and (R)-CPP ( $10 \mu$ M) to block NMDA-mediated EPSCs. **G**, Summary of the RI, calculated as  $EPSC_{60mV}/EPSC_{-60mV}$ , for AMPAR-mediated EPSCs of D1R<sup>+</sup> neurons from dominant and subordinate mice. Mann–Whitney test,  $U = 98$ ,  $*p = 0.0435$ . **H**, Sample traces of AMPAR-eEPSC at  $-60$  mV and NMDAR-eEPSC at  $+60$  mV with the presence of picrotoxin ( $50 \mu$ M) in the mPFC from dominant (red) and subordinate (blue) mice. **I**, Quantification of AMPA/NMDA ratio of D1R<sup>+</sup> neurons from dominant and subordinate mice. Mann–Whitney test,  $U = 4$ ,  $****p < 0.0001$ .

reward at the other end of the tube, a nonviolent conflict situation was created where 2 mice were released from the opposite ends of the tube and met in the middle. The mouse that forced the opponent out of the tube was identified as dominant of the pair (Fig. 1A). We ensured that the observed dominance hierarchy was stable for 3 d (Fig. 1B). We observed no difference in body weight between dominant and subordinate mice (data not shown). To characterize synaptic properties of different DA receptor-expressing neurons with respect to social rank, we performed slice recording from pairs of group-housed transgenic mice expressing red fluorescent proteins (tdTomato) under the control of the D1R or D2R promoter after classifying their social dominance status using the tube test (Figs. 1 and 2). Voltage-clamp recordings were made in visually identified D1R<sup>+</sup> or D2R<sup>+</sup> layer 5 (L5) pyramidal neurons of the PL region of the mPFC. The AMPAR-mediated miniature EPSCs (mEPSCs) were isolated by holding the neurons at the reversal potential for GABAergic currents ( $-60$  mV) with GABA<sub>A</sub>R antagonist picrotoxin ( $100 \mu$ M) and sodium channel blocker TTX ( $0.5 \mu$ M). We found that the amplitude, but not the frequency, of mEPSCs was

significantly larger in D1R<sup>+</sup> neurons from dominant mice compared with subordinates (Fig. 1D,E), suggesting that a robust postsynaptic efficacy of D1R<sup>+</sup> neurons is associated with the dominance hierarchy. In contrast, we observed neither difference in the amplitude nor frequency of mEPSCs between dominants and subordinates from D2-Tdtomato mice (Fig. 2A–C).

We further examined evoked EPSCs elicited by electrical stimulation to obtain a global overview of social dominance-related neuroplasticity. A decrease of RI of AMPAR-EPSCs (calculated as  $EPSC_{60mV}/EPSC_{-60mV}$ , RI) indicates the presence of GluA2-lacking calcium-permeable AMPARs (CP-AMPA), which are essential for AMPAR-mediated plasticity (Henley and Wilkinson, 2016). CP-AMPA are present in mature neurons, and a decrease of CP-AMPA expression in mPFC is associated with social deficits (Gascon et al., 2014). In the present study, we found that all D1R<sup>+</sup> neurons from subordinate mice exhibited  $RI > 1$  AMPAR-EPSCs (18 of 18, 100%), but  $\sim 40\%$  of D1R<sup>+</sup> neurons from dominants showed  $RI < 1$  AMPAR-EPSCs (7 of 18, 38.9%). Overall, the RI (high CP-AMPA) of D1R<sup>+</sup> neurons was significantly lower from dominant mice than that of their

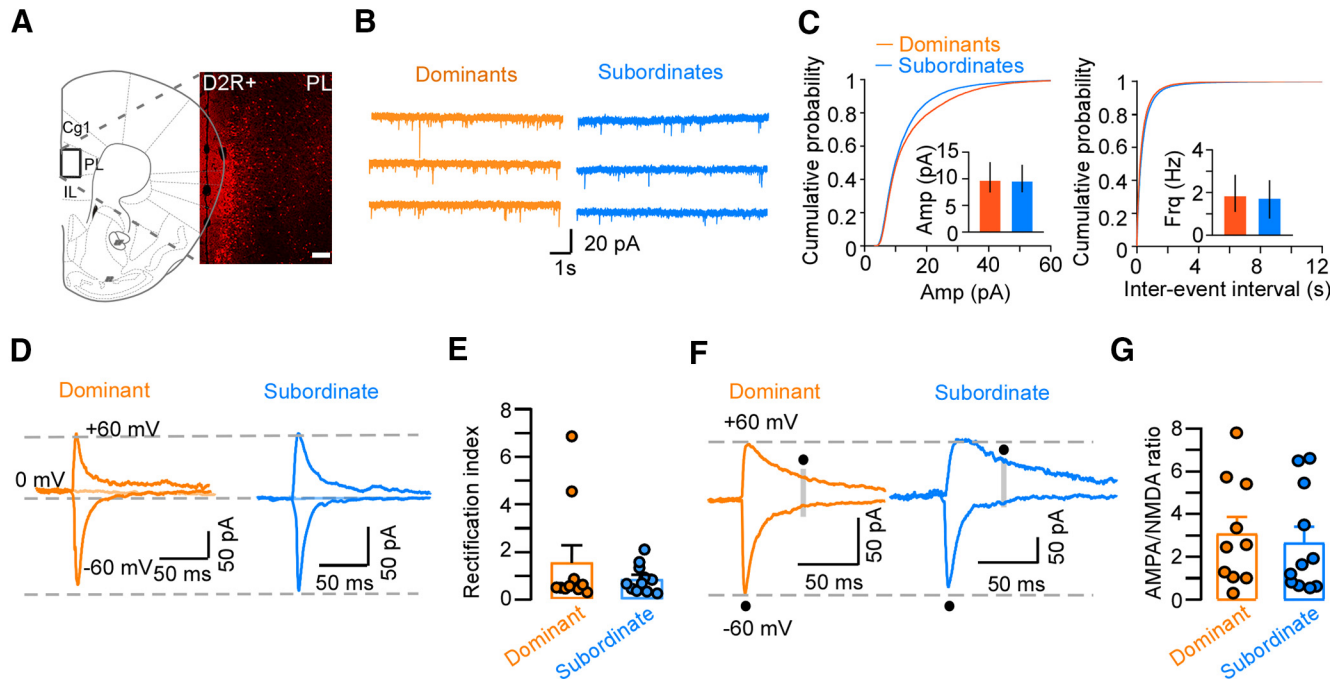


**Figure 2.** There is no difference in glutamatergic transmission in D2R<sup>+</sup> neurons in the mPFC between dominant and subordinate mice. **A**, Histologic example of mPFC from a D2R-tdTomato mouse (red, tdTomato-positive). Scale bars, 500  $\mu$ m. Cg 1, Cingulate cortex, area 1; IL, infralimbic cortex; fmi, forceps minor of the corpus callosum. **B**, Example of mEPSC recording of D2R<sup>+</sup> neurons from dominant (orange) or subordinate (light blue) mice. These experiments were conducted with the housing of 3 mice. **C**, Cumulative distribution of mEPSC amplitudes (left) and interevent intervals (right) for dominant (orange,  $n = 5$  mice) and subordinate (light blue,  $n = 5$  mice) mice. Insets, Mean ( $\pm$ SEM) mEPSC amplitude (left, Mann–Whitney test,  $U = 459$ ,  $p = 0.8843$ ) and interevent interval (right, two-tailed unpaired  $t$  test,  $t_{(59)} = 1.445$ ,  $p = 0.1538$ ). **D**, Sample traces of EPSCs at  $-60$ ,  $0$ , and  $+60$  mV in the presence of picrotoxin ( $50 \mu$ M) and (R)-CPP ( $10 \mu$ M). **E**, Summary of the RI, calculated as  $EPSC_{60mV}/EPSC_{-60mV}$ , for AMPAR-mediated EPSCs of D1R<sup>+</sup> neurons from mice with distinct ranks. Mann–Whitney test,  $U = 53$ ,  $p = 0.9177$ . **F**, Sample traces of AMPAR-eEPSC at  $-60$  mV and NMDAR-eEPSC at  $60$  mV from dominant (orange) and subordinate (light blue) D2R-tdTomato mice. **G**, Quantification of AMPA/NMDA ratio of D2R<sup>+</sup> neurons from dominant and subordinate mice. Mann–Whitney test,  $U = 48$ ,  $p = 0.6539$ .

subordinate counterparts (Fig. 1*F,G*). However, no change was observed in the RI of D2R<sup>+</sup> neurons (Fig. 2*D,E*).

The ratio of the amplitude of evoked AMPAR- and NMDAR-mediated EPSCs (AMPA/NMDA ratio), a measurement for glutamatergic synaptic strength, is a signature of plastic changes in assessing synaptic function. We found that the AMPA/NMDA ratio was significantly higher only in D1R<sup>+</sup> neurons from dominants (Fig. 1*H,I*) but not D2R<sup>+</sup> neurons (Fig. 2*F,G*). Overall, these results suggest that the more robust glutamate transmission selectively at D1R<sup>+</sup> neurons is associated with social dominance.

### Higher intrinsic excitability of D2 prefrontal neurons in subordinate mice

Prefrontal pyramidal neurons expressing DA D1Rs and D2Rs in deep layers exhibit distinct morphologic and physiological properties (Gee et al., 2012; Seong and Carter, 2012; Xing et al., 2021). We therefore compared the intrinsic membrane and action potential (AP) properties of D1R<sup>+</sup> and D2R<sup>+</sup> neurons in mPFC with respect to social rank. D1R-tdTomato and D2R-tdTomato mice were subjected to the tube test described above and then sacrificed for whole-cell current-clamp recording in pairs. The intrinsic excitability was quantified by counting the number of APs elicited by depolarizing current injections (from  $0$  to  $500$  pA; Fig. 3*A*). We found no difference in resting membrane potential between dominants and subordinates from D1R<sup>+</sup> or D2R<sup>+</sup> neurons (Fig. 3*B*; D1R<sup>+</sup> neurons). The D1R<sup>+</sup> neurons showed no difference in spike numbers between dominant mice and their subordinates (Fig. 3*C*; two-way repeated-measures ANOVA,  $F_{interaction(10,250)} = 0.3395$ ,  $p = 0.9696$ ), whereas the D2R<sup>+</sup> cells from submissive mice showed sustained hyperexcitability with

significantly higher AP numbers compared with their dominants (Fig. 3*D*).

Previous studies reported that hyperpolarization-activated cyclic nucleotide-gated (HCN) channels are localized on the distal dendrites of L5 pyramidal neurons in the mPFC, and activation of these channels decreases neural excitability (Fan et al., 2005; Li et al., 2010). Further, D2R<sup>+</sup> cells are known to be enriched with HCN channels (Gee et al., 2012; Seong and Carter, 2012), and are implicated in social deficits (Brumback et al., 2018; Yamamuro et al., 2018). We thus examined the h-current (I<sub>h</sub>, hyperpolarization-activated cation currents conducted by HCN channels) in D1R<sup>+</sup> and D2R<sup>+</sup> cells from pairs of dominant and subordinate mice by injection of hyperpolarizing current steps. Consistent with previous studies (Seong and Carter, 2012), we found that the I<sub>h</sub> is smaller in D1R<sup>+</sup> cells than in D2R<sup>+</sup> neurons in L5 of mPFC (Fig. 3*E,G*). Specifically, the I<sub>h</sub> amplitude of D2R<sup>+</sup> cells was significantly larger at  $-130$  mV (Fig. 3*F*), and these greater I<sub>h</sub>s were detected from  $-85$  to  $-130$  mV in D2R<sup>+</sup> neurons compared with D1R<sup>+</sup> (Fig. 3*G*). Furthermore, there is no observed difference of I<sub>h</sub> in D1R<sup>+</sup> cells between dominant and subordinate mice (Fig. 3*H*). In contrast, I<sub>h</sub> is significantly larger in D2R<sup>+</sup> cells of dominant mice compared with their subordinate mates (Fig. 3*H*). Together, our results suggest that increased neuronal excitability and lower I<sub>h</sub> in D2R<sup>+</sup> neurons is associated with the submissive status in social hierarchy.

### Activation of D1R neurons in the PL is required for social dominance

Thus far, our findings indicate that D1R<sup>+</sup> and D2R<sup>+</sup> pyramidal cells differ in their synaptic and physiological properties with

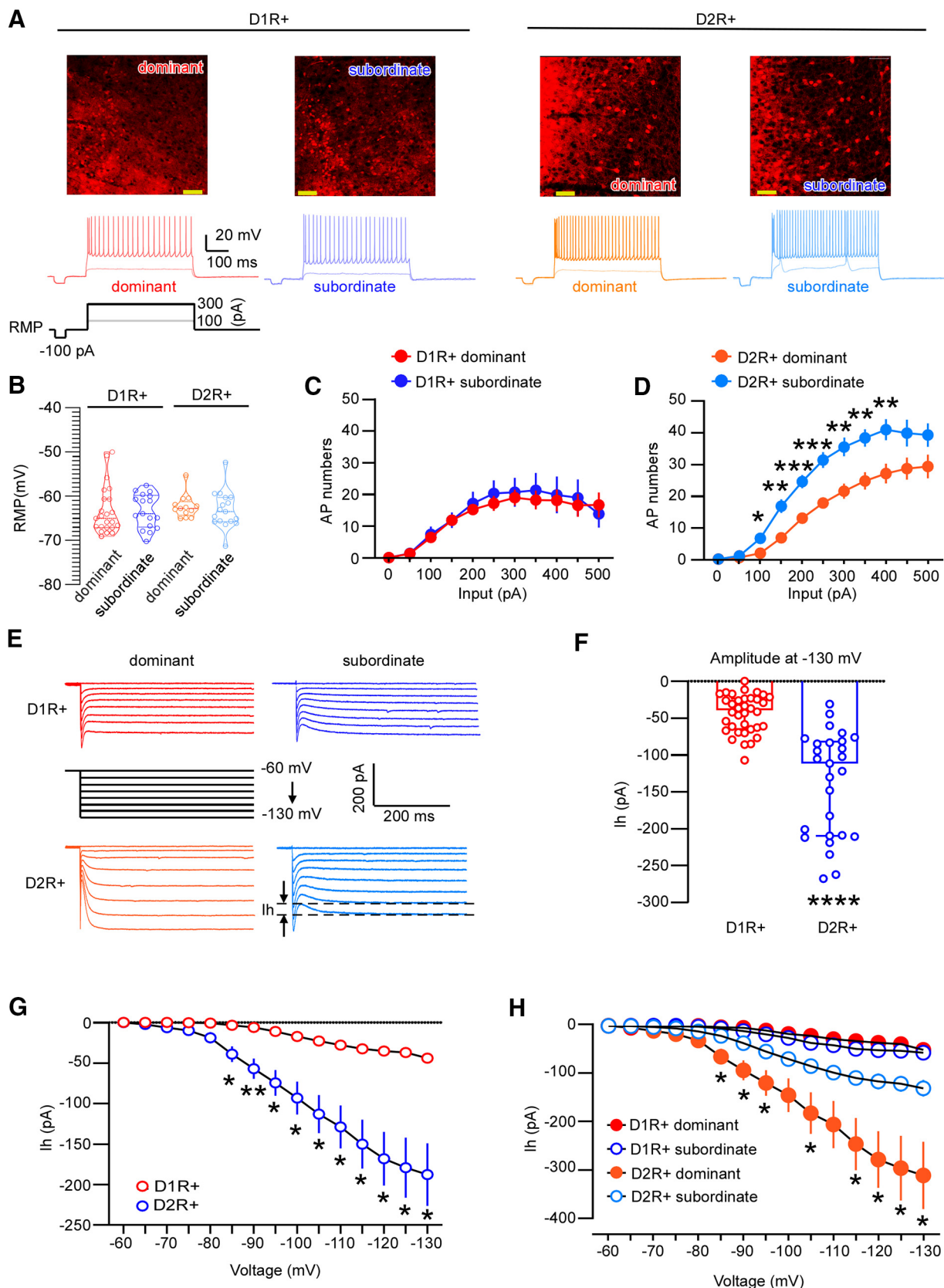


**Figure 3.** The intrinsic electrophysiological properties of L5 D1R<sup>+</sup> and D2R<sup>+</sup> pyramidal neurons in the PL of dominants and their subordinates. **A**, Example images and traces from prefrontal L5 D1R<sup>+</sup> and D2R<sup>+</sup> pyramidal neurons in response to current injections (0–500 pA at a 50 pA step, only showing 100 and 300 pA current in the sample traces for clarification) from dominant and subordinate mice after the tube test. **B**, There are no differences in rest membrane potential (RMP) in either D1R<sup>+</sup> or D2R<sup>+</sup> neurons between dominant and subordinate mice ( $n = 4$  pairs of mice). These experiments were done with the housing of 3 mice. D1R<sup>+</sup>: Mann–Whitney test,  $U = 181$ ,  $p = 0.6998$ ; D2R<sup>+</sup> neurons: two-tailed unpaired  $t$  test,  $t_{(28)} = 0.5513$ ,  $p = 0.5858$ . **C**, Quantification of the number of APs resulting from given current injections (from 0 to 500 pA) in the D1R<sup>+</sup> neurons from dominant (red) and subordinate (blue) mice. Two-way repeated-measures ANOVA, main effect of rank ( $F_{(1,25)} = 0.1026$ ,  $p = 0.7514$ ), main effect of current step ( $F_{(1,651,41,28)} = 24.49$ ,  $p < 0.0001$ ), and interaction ( $F_{(10,240)} = 0.3395$ ,  $p = 0.9696$ ). **D**, Summary of

respect to social rank. We then explored the necessity of these two types of DA receptor-expressing mPFC neurons in maintaining social hierarchy. To do this, we used inhibitory designer receptors exclusively activated by designer drugs (DREADDs) to transiently silence the activity of D1R<sup>+</sup> or D2R<sup>+</sup> neurons in mPFC during the tube test. Three weeks after stereotaxic injection of Cre-dependent AAV (AAV8-hSyn-DIO-hM4Di) into the PL region of the mPFC of D1R-Cre or D2R-Cre mice (Fig. 4A), the tube test was conducted to examine social dominance. After a stable social hierarchy was established by examining the dominance–subordinate relationship during the pretest of tube test training (Fig. 4B), dominant (defined as rank-1) and subordinate (defined as rank-3) were injected with either saline or DREADDs agonist CNO (5 mg/kg) intraperitoneally 30 min before rank testing (Fig. 4B). As controls, the middle rank (rank-2) mice received no treatment and were used to compare the rank changes with other mice. In prefrontal D1 neuron inhibition experiments, we found that inactivation of D1R<sup>+</sup> neurons (hM4Di+CNO) in dominants caused a significant drop of social rank. Notably, this effect was long-lasting for almost 8 d after CNO administration (Fig. 4C–E;  $p < 0.05$ , 24 h after injection in Test 2; and a strong trend  $p = 0.0518$ , 7 d after injection in Test 3). Importantly, the dominant D1Cre<sup>+</sup>-hM4Di mice remained in high rank with saline treatment (Fig. 4E). In contrast, inhibition of D1R<sup>+</sup> cells of subordinate mice (rank-3) did not cause any rank changes in the rank status subordinate mice (rank-3) (Fig. 4E, right). We also performed inhibitory DREADD experiments on the group of 4 mice. As shown in Figure 4F–H, we found that dominant D1Cre<sup>+</sup> mice with inhibitory hM4Di were inverted to subordinate in the group after CNO injection. Using a similar strategy, we found that silencing prefrontal D2R<sup>+</sup> neurons affect neither dominant nor subordinate status (Fig. 5).

Previous studies have indicated different cell enrichments or layer-specific expressions of D1R<sup>+</sup> and D2R<sup>+</sup> cells in the rodent mPFC. Specifically, D1Rs are the most abundant and strongly expressed in deep layers (Gaspar et al., 1995; Santana et al., 2009; Anastasiades et al., 2019). D2R<sup>+</sup> are expressed in both superficial and deep layers but are more densely enriched in superficial layers (Santana et al., 2009; Wei et al., 2018). We quantified the D1R<sup>+</sup> and D2R<sup>+</sup> cells in terms of social rank (Table 2). We

found no difference between dominants and subordinates in either D1-tdTomato or D2-tdTomato mice, but overall higher expression of D1R<sup>+</sup> than D2R<sup>+</sup> neurons in the mPFC (Table 2). While our data suggest that intact prefrontal D1R<sup>+</sup> neuronal activity is required to maintain a dominant status in a stable social hierarchy (Fig. 3C–E), we cannot rule out the possibility that the null effect of inhibiting prefrontal D2R-expressing neurons on social rank is because of its reduced abundance in deep layers of mPFC relative to D1R-expressing neurons.

### Simultaneous manipulations of D1 neurons in high-rank mice and D2 neurons in low-rank mice switch a dominance–subordination relationship

Thus far, our results suggest that enhanced synaptic strength of D1 neurons in mPFC is critical for social dominance, and hyperactivity of D2 neurons is involved in submissive status. Moreover, while we found that inactivation of D1R<sup>+</sup> prefrontal neurons caused dominant mice to adopt a subordinate social rank, inhibition of D2R<sup>+</sup> neurons did not affect social rank status in dominant or subordinate mice. We next determined whether simultaneous manipulation of D1R<sup>+</sup> and D2R<sup>+</sup> prefrontal neurons in a pair of mice could alter a dominant–subordinate relationship. Previous studies have indicated that strengthening mPFC transmission from the dorsomedial thalamus could elevate the social rank of the mice (Wang et al., 2011; Zhou et al., 2017). To this end, we expressed AAV8-DIO-hM4Di-mCherry in the mPFC of D2Cre mice to inhibit D2R<sup>+</sup> neurons (Fig. 6A) since hyperactive D2R<sup>+</sup> neurons are associated with submissive social status. To manipulate synaptic transmission onto D1 neurons, we selected mediodorsal thalamic inputs to mPFC<sup>D1</sup> synapses because synaptic strength of MD-to-mPFC is reported to maintain a dominance status (Zhou et al., 2017; Nelson et al., 2019). LTD protocols were applied to weaken the synaptic efficacy underlying social dominance. We combined a “paired training” LTD paradigm involving low-frequency light stimulation (LFS, 300 pulses of 5 ms light stimulation delivered at 1 Hz) of presynaptic inputs from the MD with a hM3Dq-induced depolarization of postsynaptic D1R<sup>+</sup> neurons in mPFC (Toyoda et al., 2005, 2007; Xing et al., 2016b). Specifically, Channelrhodopsin-2 (AAV5-CaMKII-ChR2-eYFP) and excitatory DREADD virus (AAV8-DIO-hM3Dq-mCherry) were injected into the MD and mPFC of D1Cre mice, respectively (Fig. 6B). The LFS could be delivered by blue light illumination (300 pulses of 5 ms light stimulation delivered at 1 Hz) at the MD terminals in the PL, and postsynaptic D1R<sup>+</sup> cells with hM3Dq expression were depolarized by CNO administration intraperitoneally (5 mg/kg) (Fig. 6C,D). We confirmed that LTD could be triggered at MD terminals to PL<sup>D1</sup> synapses using the “pair training” protocol in *ex vivo* slice physiological recording (Fig. 6C,D). Next, we investigated whether this “paired training” LTD protocol could suppress MD-to-PFC synapses and cause a subordinate status *in vivo*. As shown in Figure 6E, D1Cre and D2Cre mice were subjected to the tube test training paradigm after surgery. A pretest was performed to determine the dominant–subordinate relationship, and the D1Cre/dominant–D2Cre/subordinate pairs were screened to participate in the following experiments: As manipulation pair/group, the dominant D1Cre/hM3Dq/ChR2 mice received CNO injection (5 mg/kg, i.p.) 30 min before a blue light (473 nm) LFS (300 pulses of 5 ms light stimulation delivered at 1 Hz), while the subordinate D2Cre/hM4Di mice were administered CNO (5 mg/kg, i.p.) 30 min before behavioral testing. The control pair/group was set as dominants with D1Cre/mCherry/eGFP and subordinates with D2Cre/mCherry. The

←

the number of APs in response to current injections (from 0 to 500 pA) of D2R<sup>+</sup> neurons from dominant (orange) and subordinate (light blue) mice. Two-way repeated-measures ANOVA, main effect of rank ( $F_{(1,24)} = 14.35$ ,  $p = 0.0009$ ), main effect of current step ( $F_{(1,618,38.83)} = 111.1$ ,  $p < 0.0001$ ), and interaction ( $F_{(10,240)} = 3.978$ ,  $p < 0.0001$ ). Bonferroni's *post hoc* test: \* $p < 0.05$ ; \*\* $p < 0.01$ ; \*\*\* $p < 0.001$ . E, Example traces of  $-10$  mV steps showing the h-currents in response to hyperpolarizing voltage steps from  $-60$  to  $-130$  mV at a  $-5$  mV step. F, Significantly larger Ih amplitude was observed in D2R<sup>+</sup> than D1R<sup>+</sup> cell at  $-130$  mV holding voltage.  $N = 5$  pairs of mice. Mann–Whitney test,  $U = 76.5$ , \*\*\* $p < 0.0001$ . G, D2R<sup>+</sup> neurons exhibit higher Ih amplitudes than D1R<sup>+</sup> neurons from  $-85$  to  $-130$  mV voltage steps. Two-way repeated-measures ANOVA, main effect of genotype ( $F_{(1,55)} = 24.97$ ,  $p < 0.0001$ ), main effect of voltage step ( $F_{(1,158,63.69)} = 59.91$ ,  $p < 0.0001$ ), and interaction ( $F_{(14,770)} = 23.48$ ,  $p < 0.0001$ ). Bonferroni's *post hoc* test: \* $p < 0.05$ ; \*\* $p < 0.01$ . H, Summary of the Ih amplitude in response to the hyperpolarizing voltage steps recorded from D1R<sup>+</sup> and D2R<sup>+</sup> neurons in dominant versus subordinate mice, respectively. The error bars of D1R<sup>+</sup> dominant and subordinate and D2R<sup>+</sup> subordinate groups were too small to be visible in the graph. D1R<sup>+</sup>: two-way repeated-measures ANOVA, main effect of rank ( $F_{(1,34)} = 2.402$ ,  $p = 0.1305$ ), main effect of voltage step ( $F_{(1,436,48.83)} = 24.49$ ,  $p < 0.0001$ ), and interaction ( $F_{(14,476)} = 1.839$ ,  $p = 0.0309$ ). Bonferroni's *post hoc* test: all  $p > 0.05$ . D2R<sup>+</sup>: two-way repeated-measures ANOVA, main effect of rank ( $F_{(1,28)} = 8.124$ ,  $p = 0.008$ ), main effect of voltage step ( $F_{(1,183,33.13)} = 52.76$ ,  $p < 0.0001$ ), and interaction ( $F_{(14,392)} = 8.759$ ,  $p < 0.0001$ ). Bonferroni's *post hoc* test: \* $p < 0.05$ .

tube test was performed to determine the social rank and conducted for 3 consecutive days. The pairs of D1Cre/dominant-D2Cre/subordinate were subjected to three more tests at 24 h, 7 d, and 14 d later without manipulations to determine the long-term effect on the dominant–subordinate relationship. We found that weakening MD-to-PFC synaptic transmission by LTD induction in dominant mice and silencing D2R<sup>+</sup> neurons in subordinates simultaneously reversed the dominant–subordinate relationship after the 3 d manipulations in 7 of 7 pairs. In contrast, the control pairs exhibited a relatively stable D1Cre/dominant-D2Cre/subordinate relationship with only two pairs' dominant–subordinate relationship switched. Interestingly, the reversed dominance relationship in the experimental groups was stable for up to 14 d, suggesting that a brief reversal of D1R<sup>+</sup> and D2R<sup>+</sup> neuronal activities in paired mice has a long-lasting influence on their social hierarchy (Fig. 6F).

## Discussion

Our findings revealed, for the first time, that prefrontal D1 and D2 neurons play distinct but synergistic roles in social dominance. Enhanced excitatory synaptic transmission at D1 neurons is associated with dominance, and activity in prefrontal D1R-expressing neurons is required to maintain high-rank status. In contrast, hyperactive D2 neurons are associated with submissive status, and manipulating D2 neuronal excitability does not affect social rank in either dominant or submissive mice. However, simultaneous manipulation of PL D1 neurons in dominant mice and D2 neurons in subordinate mice is sufficient to switch their dominant–subordinate relationship. Moreover, this effect is long-lasting and persisting for over 2 weeks. These data indicate that activity in the D1R<sup>+</sup> and D2R<sup>+</sup> neuronal subpopulation in the mPFC regulates social hierarchy dynamics in dominant and subordinate mice.

Recent studies have shown that the mPFC is necessary and sufficient to establish a social hierarchy in mice (Wang et al., 2011; Zhou et al., 2017). During a social competition task, such as the tube test, the mean fire rate of pyramidal neurons was higher in effortful behaviors, such as push and resistance (Zhou et al., 2017). Manipulations of AMPAR-mediated currents in prefrontal pyramidal neurons bidirectionally regulate animals' positions within a social hierarchy

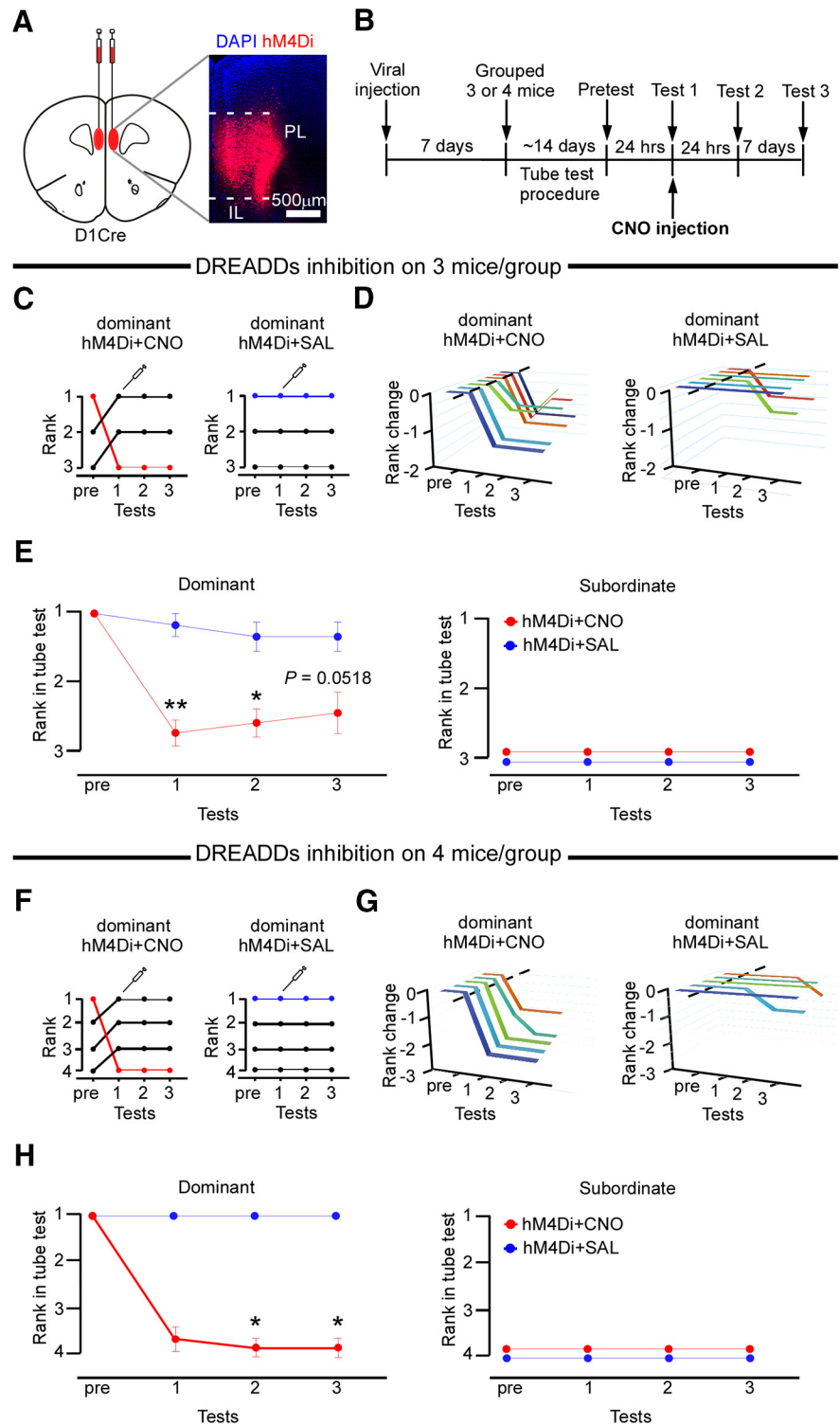


**Figure 4.** Prefrontal D1R<sup>+</sup> neuron activity is required for social dominance. **A**, Cre-dependent expression of mCherry-tagged hM4Di in D1R<sup>+</sup> neuron in the PL IL, infralimbic cortex. **B**, Experimental timeline. Mice were injected CNO (5 mg/kg, i.p.) 30 min before the first test. **C**, Social rank change of a cage (3 mice per cage) of D1 neuron hM4Di-expressing mice after CNO (left, n = 7 cages) or saline (SAL, right, n = 6 cages) treatment in the dominant. **D**, Summary of rank changes in dominant animal with D1 neuron hM4Di expression. Each line indicates 1 mouse. Dashed line indicates the injection of CNO (left) or saline control (right). **E**, Average rank change after CNO (red) or saline (blue) injection in dominant (left) and subordinate (right) D1Cre-hM4Di mice. Dominant-CNO: Friedman test,  $M_{(4)} = 17.81$ ,  $p = 0.0005$ . Dunn's *post hoc* test: \* $p < 0.05$ ; \*\* $p < 0.01$ . Dominant-Veh: Friedman test,  $M_{(4)} = 4.714$ ,  $p = 0.5$ . **F**, Social rank change of a cage (4 mice per cage) of D1 neuron hM4Di-expressing mice after CNO (left, n = 5 cages) or SAL (right, n = 5 cages) treatment in the dominant. **G**, Summary of rank changes in dominants with D1 neuron hM4Di expression for a group of 4 mice. Each line indicates 1 mouse. Dashed line indicates the injection of CNO (left) or SAL control (right). **H**, Average rank change after CNO (red) or saline (blue) injection in dominant (left) and subordinate (right) D1Cre-hM4Di mice in the group of 4 mice. Dominant-CNO: Friedman test,  $M_{(4)} = 13.91$ ,  $p = 0.0039$ . Dunn's *post hoc* test: \* $p < 0.05$ . Dominant-Veh: Friedman test,  $M_{(4)} = 4.714$ ,  $p = 0.5$ .

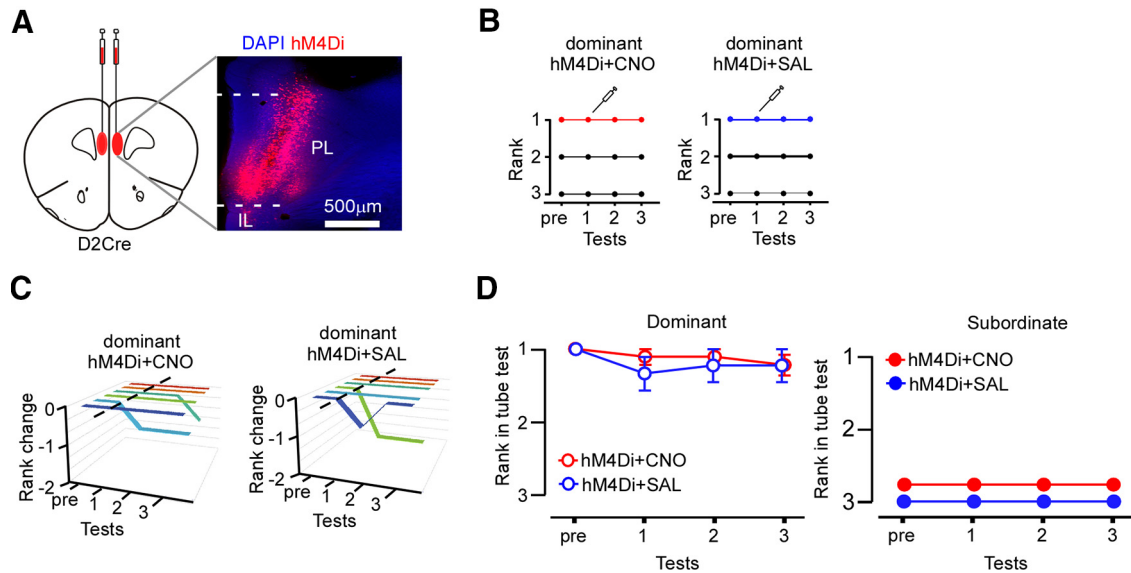


**Figure 5.** Inhibition of prefrontal D2R<sup>+</sup> neuron activity exhibited no effects on social dominance. **A**, Cre-dependent expression of mCherry-tagged hM4Di in D2R<sup>+</sup> neuron in the PL, IL, Infralimbic cortex. **B**, No social rank change in a cage of D2 neuron hM4Di-expressing mice after CNO (left,  $n = 6$  cages) or saline (SAL, right,  $n = 6$  cages) treatment in the dominant mice 30 min before Test 1. The experiments were done with the housing of 3 mice. **C**, Summary of rank changes in dominant animals with D2 neurons expressing hM4Di virus. Each line indicates 1 mouse. Dashed lines indicate the injection of CNO (left) or saline control (right) 30 min before Test 1. **D**, Rank change after CNO (red) or SAL (blue) injection in dominant (left) and subordinate (right) D2Cre mice with hM4Di expression. Dominant-CNO: Friedman test,  $M_{(4)} = 4$ ,  $p = 0.75$ . Dominant-Veh: Friedman test,  $M_{(4)} = 4$ ,  $p = 0.75$ .

**Table 2. Quantification of D1R<sup>+</sup> and D2R<sup>+</sup> cells in mPFC in the dominant–subordinate relationship and regardless of social rank**

| Group  | $n$ | Cell number (mean $\pm$ SE) |
|--|-----|-----------------------------|
| Dominant–subordinate relationship <sup>a</sup> |     |                             |
| D1R <sup>+</sup> _dominants                    | 4   | 184.3 $\pm$ 16.3            |
| D1R <sup>+</sup> _subordinates                 | 4   | 188.5 $\pm$ 18.7            |
| D2R <sup>+</sup> _dominants                    | 5   | 118.4 $\pm$ 23.3            |
| D2R <sup>+</sup> _subordinates                 | 5   | 116.4 $\pm$ 31.3            |
| Regardless of social rank <sup>b</sup>         |     |                             |
| D1R <sup>+</sup>                               | 8   | 186.4 $\pm$ 11.3            |
| D2R <sup>+</sup>                               | 10  | 117.4 $\pm$ 18.4**          |

<sup>a</sup>One-way ANOVA:  $F_{(3,17)} = 2.6134$ ,  $p = 0.0923$ , no significance.

<sup>b</sup>Unpaired  $t$  test:  $t_{(16)} = 2.9883$ ,  $p = 0.0087$ .

\*\* $p < 0.001$  versus D1R<sup>+</sup>.

(Wang et al., 2011). Consistent with these studies (Wang et al., 2011; Zhou et al., 2017), we confirmed an enhanced AMPAR-mediated synaptic transmission in layer 5 PL pyramidal neurons of dominant mice, and we show that this phenomenon mainly exists in D1R- but not D2R-expressing neurons in the mPFC (Fig. 1). D1Rs are the most abundant among the DA receptor subtypes (Gaspar et al., 1995; Santana et al., 2009), and activation of D1Rs produces excitatory effects on intrinsic excitability of deep-layer PFC pyramidal neurons (Yang and Seamans, 1996; Seong and Carter, 2012). During associative learning, D1R activation in mPFC is required to retain LTP (Gurden et al., 2000; Huang et al., 2004) and learned information (Nagai et al., 2007; Puig and Miller, 2012). Consistent with the notion that DA favors synaptic potentiation via D1R-mediated mechanisms, the AMPAR-EPSCs are selectively increased in prefrontal D1 neurons from dominants, most likely through the D1R-mediated LTP from previous winning experiences (Zhou et al., 2017). Therefore, the higher synaptic strength at D1R neurons might contribute to learning the social dominance relationships, enhancing an individual's ability to win future encounters by reinforcement learning (Kumaran et al., 2016).

Zhou et al. (2017) have demonstrated that social rank changes are positively correlated with manipulated mPFC activity, and a greater rise in rank position requiring a stronger laser intensity with optogenetics. Therefore, the distinct effect of D1 and D2 neurons inhibition on social rank revealed in our studies may be due, in part, to the number of total prefrontal cells affected. Indeed, we found overall greater expression of D1R<sup>+</sup> neurons in the mPFC relative to D2R<sup>+</sup> neurons (Table 2). In addition, we observed a laminar-specific expression difference between D1R- and D2R-expressing neurons in the mPFC. Consistent with previous studies, we found that D1Rs are the most abundant and strongly expressed in deep layers (Gaspar et al., 1995; Santana et al., 2009; Anastasiades et al., 2019), whereas D2R<sup>+</sup> are in both superficial and deep layers and more densely expressed in superficial layers (Santana et al., 2009; Wei et al., 2018). This finding raises the possibility that D2 neuron inhibition may induce a weaker effect than D1 neuron inhibition because of a relatively smaller subpopulation of prefrontal cells being manipulated.

Converging evidence shows a strong relationship between social status and psychosocial stress levels (Wang et al., 2014). Subordinate animals are prone to manifest avoidance- and anxiety-like behaviors, high glucocorticoid levels, and low immune responses when encountering a dominant intruder for a couple of days (Bartolomucci, 2007; Shinohara et al., 2018). An interesting aspect of our study was that prefrontal D2R neurons were hyperactive in the subordinate mice, who also displayed a much lower Ih than their dominant counterparts (Fig. 2). Given that activation of HCN channels decreases neuronal excitability of pyramidal neurons in deep layers (Li et al., 2010), these results suggest that hyperactivity in D2R<sup>+</sup> neurons is associated with a submissive social status. In a social context, stimulating prefrontal D2R neurons disrupts normal social interaction, while inhibiting these cells enhances social behavior in mouse models of autistic spectrum disorders (Brumback et al., 2018). Activation of D2Rs may amplify D2R<sup>+</sup> neuron responses to salient inputs, such as defeat via a Ca<sup>2+</sup> channel-dependent afterdepolarization (Gee et al., 2012).

Our findings here show that (1) synaptic strength of D1 mPFC neurons is associated with dominant status (Fig. 1) and (2) chemogenetic inhibition of D1 PFC neurons is sufficient to cause a stable switch from dominant to submissive status (Fig. 4). Although we found that D2 neurons are hyperactive in submissive mice (Fig. 3), chemogenetic inhibition of D2 neurons was not sufficient to change social rank status of the submissive mice (Fig. 5). These findings raised critical questions of whether D2R<sup>+</sup> neurons play any role in the regulation of social rank. Given our findings that inhibition of prefrontal D1 neurons can cause dominant mice to switch to submissive status, and that synaptic strength of MD inputs to the mPFC was previously identified to be crucial in maintaining a dominant social status (Zhou et al., 2017), we wondered whether inhibiting hyperactive D2R neurons in subordinate mice while simultaneously depressing synaptic transmission at MD-to-mPFC<sup>D1</sup> projections in their dominant counterparts was able to switch the social hierarchy. Interestingly, our data indicate that simultaneous manipulations of synaptic efficacy of D1 neurons in dominant mice and neuronal excitability of D2 neurons of their subordinates switch their dominant–subordinate relationship (Fig. 5). However, we cannot rule out the possibility that the behavior of the dominant mice was influenced by the activation of MD synapses on other PFC neurons. Nonetheless, these findings suggest that inhibiting hyperactive D2 neurons in submissive mice is only capable of causing a switch to dominant status when synaptic efficacy is disrupted in their dominant counterparts.

It is worth noting the different recording and stimulation methods between the present study and Zhou et al. (2017). First, we performed whole-cell patch-clamp recordings in individual pyramidal neurons in the mPFC (Fig. 6C,D), whereas Zhou et al. (2017) measured local field potentials (fEPSPs) in a population of mPFC cells for the LTD experiments. Second, different protocols to induce LTD were used. Specifically, we found that optogenetic stimulation of presynaptic MD-to-mPFC pathway (with 300 1 Hz pulses of 5 ms duration) paired with postsynaptic depolarization of D1R<sup>+</sup> neurons using chemogenetics induced robust LTD in MD-to-mPFC<sup>D1</sup> synapses. In contrast, Zhou et al. (2017) used optogenetic

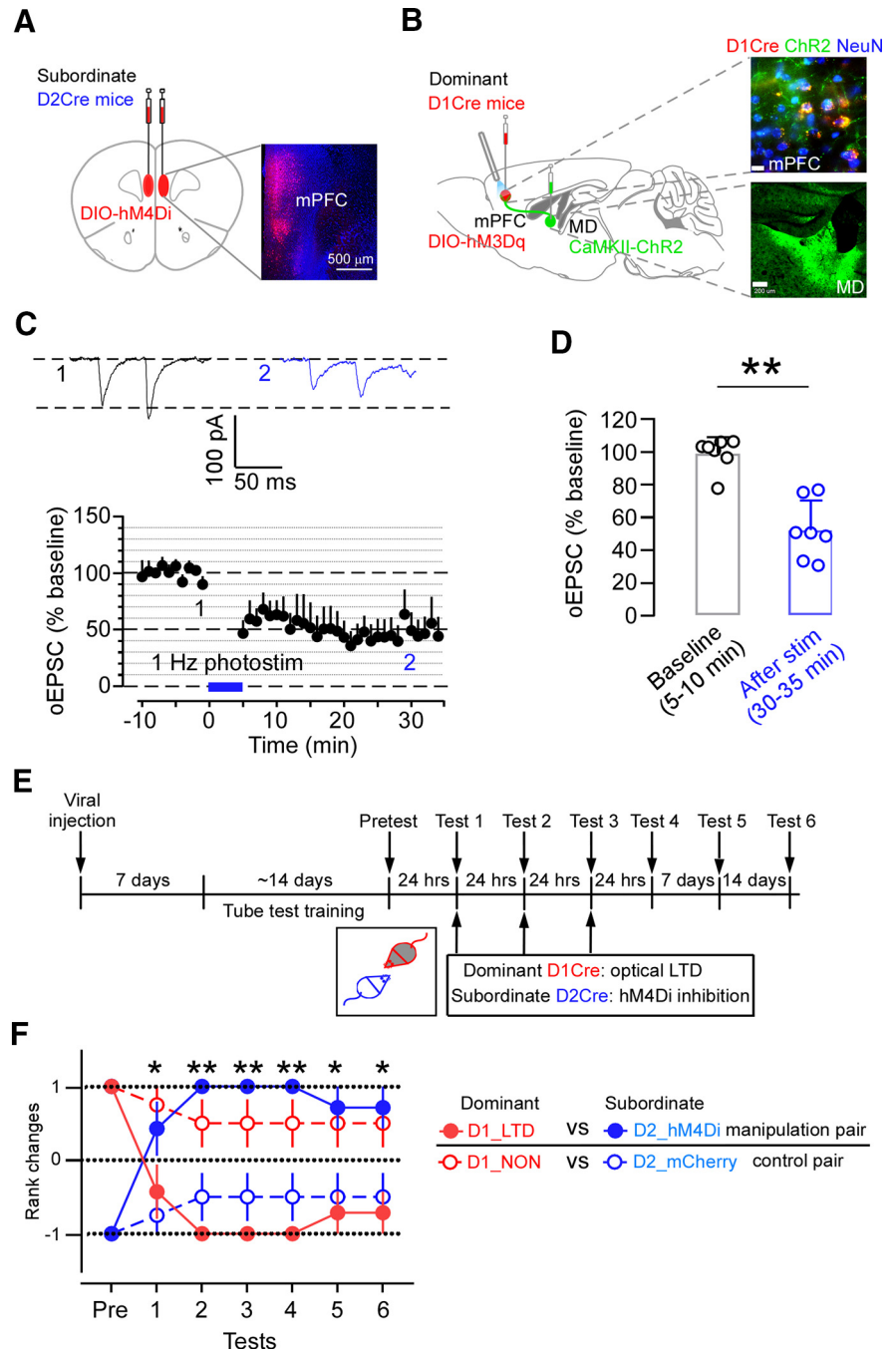


**Figure 6.** Simultaneous manipulation of prefrontal D1R<sup>+</sup> neurons in dominants and D2R<sup>+</sup> neurons in subordinates switches their dominance–subordinate relationship. **A**, Viral transduction of D2R<sup>+</sup> neurons with hM4Di in mPFC of subordinate D2Cre mice. **B**, A combined viral approach of transduction of D1R<sup>+</sup> neurons with hM3Dq in mPFC and Chr2 in the MD in dominant D1Cre mice. The experiments were done with the housing of 2 mice. **C**, Using a combined approach of low-frequency blue light stimulation (LFS, 300 pulses at 1 Hz, 473 nm, 8 mW) with depolarization of D1R<sup>+</sup> cells by hM3Dq/CNO, LTD was induced at MD–mPFC synapses in D1R<sup>+</sup> neurons. Top, Example traces of optical stimulation-evoked EPSC (oEPSC) before (black) and after (blue) LTD protocol application. Bottom, Time course of oEPSC change before and after LTD protocol application, EPSC amplitude was normalized to the baseline. **D**, There is a significant reduction of oEPSCs amplitude after LTD protocol application.  $n = 7$  from 3 mice. Two-tailed paired  $t$  test,  $t_{(6)} = 6.032$ ,  $**p = 0.0009$ . **E**, Schematic of the experimental design and tube test procedure and timeline used to test whether simultaneous manipulation of D1R<sup>+</sup> and D2R<sup>+</sup> neurons in the PL region of mPFC alters dominance–subordinate relationship in a pair of mice ( $n = 7$  manipulation pairs,  $n = 8$  control pairs). **F**, Summary of the average rank change before (pretest), during (Tests 1–3), and after (Tests 4–6) the simultaneous manipulations of prefrontal D1R<sup>+</sup> and D2R<sup>+</sup> neurons. The dominant rank was set as 1, and the subordinate rank was set as  $-1$ . The rank changes of dominant–subordinate relationship from pretest to Test 6 were plotted. Fisher’s exact test:  $*p = 0.0406$  at Tests 1, 5, and 6,  $**p = 0.007$  at Tests 2, 3 and 4.

stimulation of MD terminals to induce LTD at MD-to-mPFC synapses with an application of 900 1 Hz pulses of 2 ms duration. Since we used 300 instead of 900 presynaptic stimulations, we expect no LTD induction without a postsynaptic depolarization. These differences in recording methods would likely result in different findings that need further exploration. Despite the methodological differences, both our findings and those from Zhou et al. (2017) support the idea that weakening synaptic efficacy of MD-PFC synapses diminishes a dominant social status.

A recent study demonstrated that mice engaging in a dominance test show interbrain synchrony, which emerges from mPFC neurons encoding of self-behaviors and those of their social partners. Interestingly, self-behaviors were more strongly encoded in dominant mice, whereas opponent behaviors were more strongly encoded in submissive mice (Kingsbury et al., 2019). Given our findings that D1 and D2 neurons play distinct roles based on social status, an intriguing aspect for future study will be to determine whether and how these neurons may contribute to the differential computational structure mPFC circuits in dominant and submissive mice. Because prefrontal DA plays a critical role in the regulation of adaptive social behaviors and decision-making (St Onge et al., 2011; Brumback et al., 2018; Lee et al., 2018), novel tools that can detect relative DA levels with high spatiotemporal resolution will be critical to further understand how DA signals modulate ongoing social activities via the segregated D1R- and D2R-dominant networks (Sun et al., 2018).

In conclusion, our findings provide novel insight into the divergent functions of prefrontal D1R and D2R neurons in social dominance. The D1 and D2 neurons within mPFC work synergistically to regulate social hierarchy via different neuroplasticity mechanisms.

## References

- Anastasiades PG, Boada C, Carter AG (2019) Cell type-specific d1 dopamine receptor modulation of projection neurons and interneurons in the prefrontal cortex. *Cereb Cortex* 29:3224–3242.
- Arnsten AF (2009) Stress signalling pathways that impair prefrontal cortex structure and function. *Nat Rev Neurosci* 10:410–422.
- Bartolomucci A (2007) Social stress, immune functions and disease in rodents. *Front Neuroendocrinol* 28:28–49.
- Bicks LK, Koike H, Akbarian S, Morishita H (2015) Prefrontal cortex and social cognition in mouse and man. *Front Psychol* 6:1805.
- Blanchard RJ, McKittrick CR, Blanchard DC (2001) Animal models of social stress: effects on behavior and brain neurochemical systems. *Physiol Behav* 73:261–271.
- Brumback AC, Ellwood IT, Kjaerby C, Iafraji J, Robinson S, Lee AT, Patel T, Nagaraj S, Davatolhagh F, Sohal VS (2018) Identifying specific prefrontal neurons that contribute to autism-associated abnormalities in physiology and social behavior. *Mol Psychiatry* 23:2078–2089.
- Chiao JY (2010) Neural basis of social status hierarchy across species. *Curr Opin Neurobiol* 20:803–809.
- de Almeida RM, Ferrari PF, Parmigiani S, Miczek KA (2005) Escalated aggressive behavior: dopamine, serotonin and GABA. *Eur J Pharmacol* 526:51–64.
- Draws C (1993) The concept and definition of dominance in animal behaviour. *Behaviour* 125:283–313.
- Ernst M, Zametkin A, Matochik J, Pascualvaca D, Cohen R (1997) Low medial prefrontal dopaminergic activity in autistic children. *Lancet* 350:638.
- Fan Y, Fricker D, Brager DH, Chen X, Lu HC, Chitwood RA, Johnston D (2005) Activity-dependent decrease of excitability in rat hippocampal neurons through increases in I(h). *Nat Neurosci* 8:1542–1551.
- Franklin TB, Silva BA, Perova Z, Marrone L, Masferrer ME, Zhan Y, Kaplan A, Greetham L, Verrechia V, Halman A, Pagella S, Vyssotski AL, Illarionova A, Grinevich V, Branco T, Gross CT (2017) Prefrontal cortical control of a brainstem social behavior circuit. *Nat Neurosci* 20:260–270.
- Gascon E, Lynch K, Ruan H, Almeida S, Verheyden JM, Seeley WW, Dickson DW, Petrucelli L, Sun D, Jiao J, Zhou H, Jakovcevski M, Akbarian S, Yao WD, Gao FB (2014) Alterations in microRNA-124 and AMPA receptors contribute to social behavioral deficits in frontotemporal dementia. *Nat Med* 20:1444–1451.
- Gaspar P, Bloch B, Le Moine C (1995) D1 and D2 receptor gene expression in the rat frontal cortex: cellular localization in different classes of efferent neurons. *Eur J Neurosci* 7:1050–1063.
- Ge S, Ellwood I, Patel T, Luongo F, Deisseroth K, Sohal VS (2012) Synaptic activity unmasks dopamine D2 receptor modulation of a specific class of layer V pyramidal neurons in prefrontal cortex. *J Neurosci* 32:4959–4971.
- Gurden H, Takita M, Jay TM (2000) Essential role of D1 but not D2 receptors in the NMDA receptor-dependent long-term potentiation at hippocampal-prefrontal cortex synapses in vivo. *J Neurosci* 20:RC106.
- Henley JM, Wilkinson KA (2016) Synaptic AMPA receptor composition in development, plasticity and disease. *Nat Rev Neurosci* 17:337–350.
- Huang YY, Simpson E, Kellendonk C, Kandel ER (2004) Genetic evidence for the bidirectional modulation of synaptic plasticity in the prefrontal cortex by D1 receptors. *Proc Natl Acad Sci USA* 101:3236–3241.
- Kingsbury L, Huang S, Wang J, Gu K, Golshani P, Wu YE, Hong W (2019) Correlated neural activity and encoding of behavior across brains of socially interacting animals. *Cell* 178:429–446.e416.
- Kumaran D, Banino A, Blundell C, Hassabis D, Dayan P (2016) Computations underlying social hierarchy learning: distinct neural mechanisms for updating and representing self-relevant information. *Neuron* 92:1135–1147.
- Lee YA, Lionnet S, Kato A, Goto Y (2018) Dopamine-dependent social information processing in non-human primates. *Psychopharmacology (Berl)* 235:1141–1149.
- Levy DR, Tamir T, Kaufman M, Parabucki A, Weissbrod A, Schneidman E, Yizhar O (2019) Dynamics of social representation in the mouse prefrontal cortex. *Nat Neurosci* 22:2013–2022.
- Li B, Chen F, Ye J, Chen X, Yan J, Li Y, Xiong Y, Zhou Z, Xia J, Hu Z (2010) The modulation of orexin A on HCN currents of pyramidal neurons in mouse prefrontal cortex. *Cereb Cortex* 20:1756–1767.
- Li YC, Panikker P, Xing B, Yang SS, Alexandropoulos C, McEachern EP, Akumuo R, Zhao E, Gulchina Y, Pletnikov MV, Urs NM, Caron MG, Elefant F, Gao WJ (2020) Deletion of glycogen synthase kinase-3beta in D2 receptor-positive neurons ameliorates cognitive impairment via NMDA receptor-dependent synaptic plasticity. *Biol Psychiatry* 87:745–755.
- Matthews GA, Tye KM (2019) Neural mechanisms of social homeostasis. *Ann NY Acad Sci* 1457:5–25.
- Nagai T, Takuma K, Kamei H, Ito Y, Nakamichi N, Ibi D, Nakanishi Y, Murai M, Mizoguchi H, Nabeshima T, Yamada K (2007) Dopamine D1 receptors regulate protein synthesis-dependent long-term recognition memory via extracellular signal-regulated kinase 1/2 in the prefrontal cortex. *Learn Mem* 14:117–125.
- Nelson AC, Kapoor V, Vaughn E, Gnanasegaram J, Rubinstein N, Murthy VN, Dulac C (2019) Molecular and circuit architecture of social hierarchy. *bioRxiv*. doi: <https://doi.org/10.1101/838664>.
- Nelson RJ, Trainor BC (2007) Neural mechanisms of aggression. *Nat Rev Neurosci* 8:536–546.
- Phillips ML, Robinson HA, Pozzo-Miller L (2019) Ventral hippocampal projections to the medial prefrontal cortex regulate social memory. *Elife* 8:e44182.
- Puig MV, Miller EK (2012) The role of prefrontal dopamine D1 receptors in the neural mechanisms of associative learning. *Neuron* 74:874–886.
- Rangel A, Camerer C, Montague PR (2008) A framework for studying the neurobiology of value-based decision making. *Nat Rev Neurosci* 9:545–556.
- Rose RM, Holaday JW, Bernstein IS (1971) Plasma testosterone, dominance rank and aggressive behaviour in male rhesus monkeys. *Nature* 231:366–368.
- Santana N, Mengod G, Artigas F (2009) Quantitative analysis of the expression of dopamine D1 and D2 receptors in pyramidal and GABAergic neurons of the rat prefrontal cortex. *Cereb Cortex* 19:849–860.
- Sapolsky RM (2005) The influence of social hierarchy on primate health. *Science* 308:648–652.
- Seong HJ, Carter AG (2012) D1 receptor modulation of action potential firing in a subpopulation of layer 5 pyramidal neurons in the prefrontal cortex. *J Neurosci* 32:10516–10521.

- Shinohara R, Taniguchi M, Ehrlich AT, Yokogawa K, Deguchi Y, Cherasse Y, Lazarus M, Urade Y, Ogawa A, Kitaoka S, Sawa A, Narumiya S, Furuyashiki T (2018) Dopamine D1 receptor subtype mediates acute stress-induced dendritic growth in excitatory neurons of the medial prefrontal cortex and contributes to suppression of stress susceptibility in mice. *Mol Psychiatry* 23:1717–1730.
- Sparta DR, Stamatakis AM, Phillips JL, Hovelso N, van Zessen R, Stuber GD (2011) Construction of implantable optical fibers for long-term optogenetic manipulation of neural circuits. *Nat Protoc* 7:12–23.
- St Onge JR, Abhari H, Floresco SB (2011) Dissociable contributions by prefrontal D1 and D2 receptors to risk-based decision making. *J Neurosci* 31:8625–8633.
- Stagkourakis S, Spigolon G, Williams P, Protzmann J, Fisone G, Broberger C (2018) A neural network for intermale aggression to establish social hierarchy. *Nat Neurosci* 21:834–842.
- Sun F, Zeng J, Jing M, Zhou J, Feng J, Owen SF, Luo Y, Li F, Wang H, Yamaguchi T, Yong Z, Gao Y, Peng W, Wang L, Zhang S, Du J, Lin D, Xu M, Kreitzer AC, Cui G, et al. (2018) A genetically encoded fluorescent sensor enables rapid and specific detection of dopamine in flies, fish, and mice. *Cell* 174:481–496.e419.
- Toyoda H, Wu LJ, Zhao MG, Xu H, Jia Z, Zhuo M (2007) Long-term depression requires postsynaptic AMPA GluR2 receptor in adult mouse cingulate cortex. *J Cell Physiol* 211:336–343.
- Toyoda H, Zhao MG, Zhuo M (2005) Roles of NMDA receptor NR2A and NR2B subtypes for long-term depression in the anterior cingulate cortex. *Eur J Neurosci* 22:485–494.
- Tritsch NX, Sabatini BL (2012) Dopaminergic modulation of synaptic transmission in cortex and striatum. *Neuron* 76:33–50.
- van Aerde KI, Feldmeyer D (2015) Morphological and physiological characterization of pyramidal neuron subtypes in rat medial prefrontal cortex. *Cereb Cortex* 25:788–805.
- Vander Weele CM, Siciliano CA, Matthews GA, Namburi P, Izadmehr EM, Espinel IC, Nieh EH, Schut EH, Padilla-Coreano N, Burgos-Robles A, Chang CJ, Kimchi EY, Beyeler A, Wichmann R, Wildes CP, Tye KM (2018) Dopamine enhances signal-to-noise ratio in cortical-brainstem encoding of aversive stimuli. *Nature* 563:397–401.
- Wang F, Zhu J, Zhu H, Zhang Q, Lin Z, Hu H (2011) Bidirectional control of social hierarchy by synaptic efficacy in medial prefrontal cortex. *Science* 334:693–697.
- Wang F, Kessels HW, Hu H (2014) The mouse that roared: neural mechanisms of social hierarchy. *Trends Neurosci* 37:674–682.
- Wei X, Ma T, Cheng Y, Huang CC, Wang X, Lu J, Wang J (2018) Dopamine D1 or D2 receptor-expressing neurons in the central nervous system. *Addict Biol* 23:569–584.
- Williamson CM, Lee W, Curley JP (2016) Temporal dynamics of social hierarchy formation and maintenance in male mice. *Anim Behav* 115:259–272.
- Xing B, Li YC, Gao WJ (2016a) Norepinephrine versus dopamine and their interaction in modulating synaptic function in the prefrontal cortex. *Brain Res* 1641:217–233.
- Xing B, Li YC, Gao WJ (2016b) GSK3beta hyperactivity during an early critical period impairs prefrontal synaptic plasticity and induces lasting deficits in spine morphology and working memory. *Neuropsychopharmacology* 41:3003–3015.
- Xing B, Han G, Wang MJ, Snyder MA, Gao WJ (2018) Juvenile treatment with mGluR2/3 agonist prevents schizophrenia-like phenotypes in adult by acting through GSK3beta. *Neuropharmacology* 137:359–371.
- Xing B, Mack NR, Guo KM, Zhang YX, Ramirez B, Yang SS, Lin L, Wang DV, Li YC, Gao WJ (2021) A subpopulation of prefrontal cortical neurons is required for social memory. *Biol Psychiatry* 89:521–531.
- Xu TX, Yao WD (2010) D1 and D2 dopamine receptors in separate circuits cooperate to drive associative long-term potentiation in the prefrontal cortex. *Proc Natl Acad Sci USA* 107:16366–16371.
- Yamamoto K, Yoshino H, Ogawa Y, Makinodan M, Toritsuka M, Yamashita M, Corfas G, Kishimoto T (2018) Social isolation during the critical period reduces synaptic and intrinsic excitability of a subtype of pyramidal cell in mouse prefrontal cortex. *Cereb Cortex* 28:998–1010.
- Yang CR, Seamans JK (1996) Dopamine D1 receptor actions in layers V–VI rat prefrontal cortex neurons in vitro: modulation of dendritic-somatic signal integration. *J Neurosci* 16:1922–1935.
- Yang SS, Li YC, Coley AA, Chamberlin LA, Yu P, Gao WJ (2018) Cell-type specific development of the hyperpolarization-activated current, Ih, in prefrontal cortical neurons. *Front Synaptic Neurosci* 10:7.
- Zhou T, Zhu H, Fan Z, Wang F, Chen Y, Liang H, Yang Z, Zhang L, Lin L, Zhan Y, Wang Z, Hu H (2017) History of winning remodels thalamo-PFC circuit to reinforce social dominance. *Science* 357:162–168.
- Zhou T, Sandi C, Hu H (2018) Advances in understanding neural mechanisms of social dominance. *Curr Opin Neurobiol* 49:99–107.
- Zink CF, Tong Y, Chen Q, Bassett DS, Stein JL, Meyer-Lindenberg A (2008) Know your place: neural processing of social hierarchy in humans. *Neuron* 58:273–283.